Nat. Hazards Earth Syst. Sci., 11, 1233–1246, 2011
www.nat-hazards-earth-syst-sci.net/11/1233/2011/
doi:10.5194/nhess-11-1233-2011

Natural Hazards and Earth System Sciences

Numerical simulation of a deep Mediterranean storm and its sensitivity on sea surface temperature

P. Katsafados[1], **E. Mavromatidis**[1], **A. Papadopoulos**[2], **and I. Pytharoulis**[3]

[1]Department of Geography, Harokopio University of Athens, 70 El. Venizelou Str., P.O. Box 17671, Athens, Greece
[2]Institute of Inland Waters, Hellenic Centre for Marine Research, P.O. Box 712, 19013, Anavyssos Attikis, Greece
[3]Department of Meteorology and Climatology, School of Geology, Aristotle University of Thessaloniki, P.O. Box 54124, Thessaloniki, Greece

Received: 14 May 2010 – Revised: 4 February 2011 – Accepted: 3 March 2011 – Published: 3 May 2011

Abstract. The development and evolution of a deep low-pressure system over the Eastern Mediterranean has been investigated in comparative numerical experiments with a limited area model using climatological, gridded analyses, satellite-derived and high-resolution re-analysis sea surface temperatures (SSTs) as lower boundary conditions. The severe event of 21–22 January 2004 was selected in view of its strength and considerable impact on the coastal communities of the Northern Aegean Sea. The aim of this study is to investigate the sensitivity of storm development and intensity to the different SST sources. High resolution model simulations were performed resolving mesoscale features modulated by the different source of SSTs. Although the atmospheric response was considerable in terms of rain bands and surface fluxes, the general structure of the system was not significantly affected by the different air-sea interaction forcing. The impact on the model performance (and therefore its forecasting skill) was further assessed on the basis of quantitative verification statistics estimated throughout the period of the simulations. The methodology was based on the verification against surface observations from the World Meteorological Organization network, covering Southern Greece and the coastal areas of Western Turkey. The estimated statistical scores revealed small but noticeable deviations among the forecast skills of the simulations.

Correspondence to: P. Katsafados
(pkatsaf@hua.gr)

1 Introduction

A complicated matter in current meteorological research is the explanation of explosive cyclogenesis's tendency to occur preferably in wintertime, marine environments and in regions of strong sea surface temperature (SST) gradients ($\sim$10 °C per 180 km). During the eighties, much attention in synoptic meteorology was devoted to the special class of extratropical cyclones that develop at an unusually rapid rate. The first synoptic climatological study of such explosively developing storm or "bomb" has been documented by Sanders and Gyakum (1980), who define an extratropical cyclone as a bomb when the mean sea-level pressure of its center falls by at least 1 hPa per hour for 24 h at 60° N. An equivalent rate is obtained for a latitude ϕ by multiplying this rate by the dimensionless number $\sin\phi/\sin 60°$. Sanders and Gyakum (1980) denote this threshold rate as one bergeron. In addition to the abovementioned study, various authors have investigated the contribution of the synoptic environment, as well as the role of the surface features (e.g. surface fluxes, SST databases) in the explosive cyclogenesis (Sanders, 1986; Gyakum and Danielson, 2000; Strahl and Smith, 2001; Rouault et al., 2002; Martin and Otkin, 2004; Hirose and Fukudome, 2006). According to Sanders (1986), strong bombs reach their most rapid deepening rates upon crossing regions of high SST gradients, while, Pandolfo (1985) claims that, rapid cyclogenesis occurs mainly over oceans due to the differences between marine and continental environments. Minobe at al. (2008) in turn, investigated the Gulf Stream impacts on the troposphere and revealed that in the marine boundary layer, atmospheric

Published by Copernicus Publications on behalf of the European Geosciences Union.

pressure adjustments to sharp sea surface temperature gradients lead to surface wind convergence that anchors a narrow precipitation band along the Gulf Stream. In this rain band, upward motions and cloud formation extend into the upper troposphere as corroborated by the frequent occurrence of very cold cloud-top temperatures. These mechanisms offer a direct pathway, by which the Gulf Stream can affect the atmosphere both locally and possibly in remote regions via planetary wave propagation.

Recent modeling studies seem to suggest different roles of the SST and heat flux in forcing the extratropical atmosphere (Kushnir et al., 2002; Yulaeva et al., 2001; Sutton and Mathieu, 2002; Liu and Wu, 2004). Arguing along these lines, Yamamoto and Hirose (2007) as well as Kathleen and Capehart (2008) have demonstrated that model simulations are sensitive to the SST input data. Namely, SSTs can significantly affect a given forecast based on its spatial and temporal resolution and its original source (e.g. observed, model derived or based on climatology). Rouault et al. (2003) examined the ability of operational models from the National Centers for Environmental Prediction (NCEP) and the European Centre for Medium Range Weather Forecasts (ECMWF) to adequately resolve the air-sea heat fluxes in the Agulhas Current region (South Africa). They suggested that high resolution is needed, due to the tight gradients in SST between the Agulhas Current core and ambient waters. In the Mediterranean basin, Lebeaupin et al. (2009) investigated the mesoscale ocean response and its sensitivity to the time resolution of the atmospheric forcing. They concluded that the Mediterranean is a region propitious to severe weather conditions including intense air – sea exchanges, such as strong local winds and intense cyclogenesis.

The occurrence of a meteorological bomb in the Mediterranean Sea is not a rare phenomenon. A review of this kind of cyclones in the Mediterranean basin has been provided by Conte et al. (2002). Their statistical analysis indicates that most of these events occur in the central Mediterranean with a secondary maximum appearing over the Aegean Sea. Capaldo et al. (1980), as well as Karacostas and Flocas (1983), having investigated the dynamic processes involved in bomb development in the Mediterranean Sea, put forward two fundamental types. In the first type, the bomb develops from an interaction between a baroclinic, open long wave and an unstable short wave. The resulting cyclonic vorticity, the upper air temperature advection and the sensible and latent heat exchange support the rapid and intense deepening of the system. In the second type, the bomb originates from the interaction between a synoptic mid-latitude depression, deeply penetrated into the Mediterranean, and a sub-synoptic depression of African origin. Often, the interaction can be an effective intrusion of an African depression into a larger scale low-pressure area drawn from middle latitudes. In this process the low-level jet-stream and the intense baroclinicity assume highly important roles, related to the strong thermal contrast between the two systems of quite different origins. Based on these studies Conte et al. (2002) pointed out the relevant importance of the Mediterranean SSTs in both types of development and concluded that the bomb is essentially a meteo-marine phenomenon. Lagouvardos et al. (1999) investigated the importance of the surface fluxes in the development of a sub-synoptic vortex with the characteristics of a tropical storm in the Mediterranean. The numerical experiments showed that the triggering mechanism for the vortex genesis was the synergy of the low level baroclinicity and the existence of a mid-tropospheric cut-off low while during the mature stage of the vortex, latent-heat release within the convective motions was the dominant mechanism which sustained the vortex until its landfall. Pastor et al. (2001) studied 32 torrential rains near the Spanish Mediterranean Coast. Their analysis based on the National Oceanic and Atmospheric Administration (NOAA) satellite images and the trajectories of the surface air masses indicated that the Mediterranean SST along the rain paths drops by 3–5 °C with respect to prior values. The reduction in the observed SST following the event has mainly been the result of vigorous evaporative cooling along the back door front. For Millán et al. (1995), thereby, the warmer areas of the Mediterranean acted as a source of moisture for the torrential episodes. The authors considered that sea water temperature is one of the key factors in determining the onset of the torrential precipitations, both in their genesis and, once they have started, in the amount of rain fallen.

In the present study, comparative numerical simulations of a deep Mediterranean storm in marine environment have been performed with a non-hydrostatic atmospheric model. Climatological, gridded analyses, satellite-derived and high-resolution re-analysis SSTs were applied as lower boundary conditions. Furthermore, an additional experiment has been conducted in order to assess the sensitivity of the system on an extreme and non-realistic surface forcing. This study in fact aims at determining the sensitivity of precipitation and storm intensity to various realistic and non-realistic SST patterns. The incident of 21–22 January 2004 was thereby selected as a case study, due to its intensity and significant effects upon the coastal areas of Northern Aegean Sea and the Eastern Mediterranean in general. According to the MEDEX database (MEDiteranean Experiment), this event has been classified as one of the three deepest cyclones affecting the Mediterranean over the last 40 years and has been characterized as a meteorological bomb (Lagouvardos et al., 2007). The variable effect of lower boundary conditions on the model performance is further examined via quantitative verification statistics based on simulated meteorological fields and surface observations from the World Meteorological Organization (WMO) network.

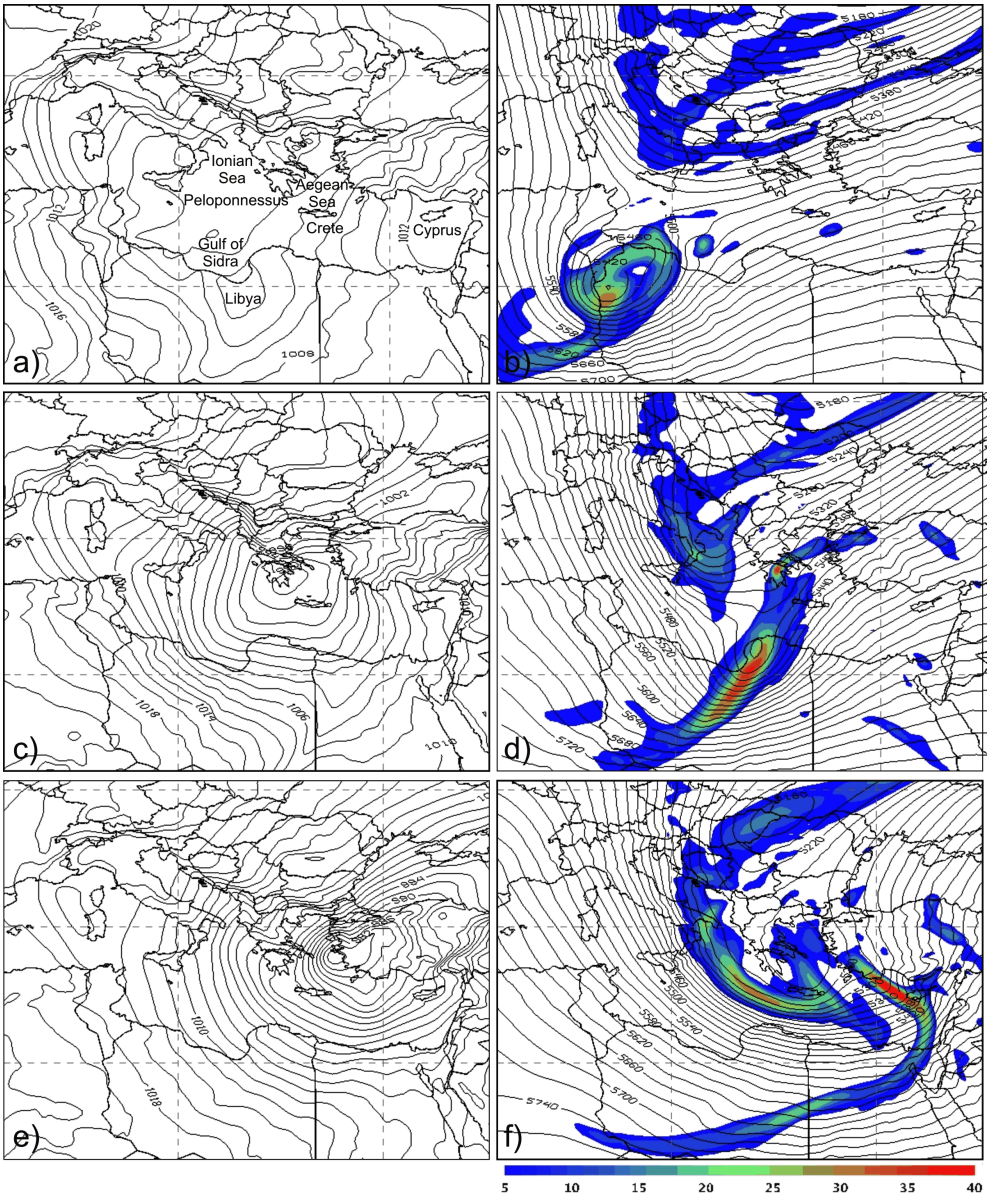

Fig. 1. (a) Mean sea level pressure (MSLP) in hPa at 12:00 UTC, 21 January 2004, **(b)** geopotential height (solid lines) at 500 hPa with absolute vorticity (colour shaded; only values greater than $5.0\times10^{-5}\,s^{-1}$ are shown) at 12:00 UTC, 21 January 2004, **(c)** MSLP at 00:00 UTC, 22 January 2004, **(d)** geopotential height at 500 hPa with absolute vorticity at 00:00 UTC, 22 January 2004, **(e)** MSLP at 12:00 UTC, 22 January 2004, and **(f)** geopotential height at 500 hPa with absolute vorticity at 12:00 UTC, 22 January 2004. The entire fields are based on ECMWF analyses

.

2 Description of the synoptic conditions

The investigation of the prevailing synoptic conditions during storm formation and evolution is based on the analysis fields of the ECMWF at a horizontal resolution of $0.50°\times0.50°$ and a temporal increment of 6 h. According to the ECMWF analysis, surface cyclogenesis began at about 12:00 UTC on 21 January 2004 in the Gulf of Sidra with central mean sea level pressure of 998.9 hPa (Fig. 1a). The precursor of the surface cyclone was a cut-off low located over Libya (Fig. 1b). Figure 1b further indicates the areas where the absolute vorticity exceeds the threshold of $5.0\times10^{-5}\,s^{-1}$ at 500 hPa. The fact that the maximum absolute vorticity at 500 hPa ($\sim30.0\times10^{-5}\,s^{-1}$) at the time was located west of the surface cyclone, strongly indicates the rapid baroclinic development. According to the literature (Sanders, 1986), high absolute vorticity maximum at 500 hPa which exists upstream, and prior to the surface cyclone, interacts with the

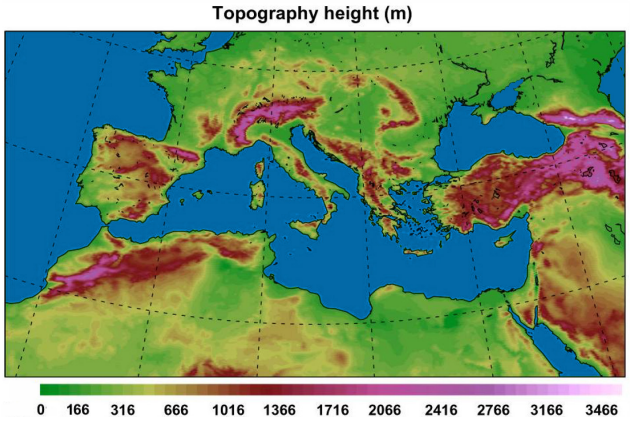

Fig. 2. The integration domain and the resolved topography (m) for the entire experiments referred in this study.

storm (in the most of the cases) at the time when the explosive development is triggered. In addition MacDonald and Reiter (1988) report that during the explosive phase, a 500 hPa vorticity maximum is located about 500 km west of the surface position of the storm center.

The system deepened further at a rate of 13.2 hPa during a 12 h period (from 12:00 UTC, 21 January to 00:00 UTC, 22 January) and moved over the southern part of the Greek Peninsula. Its central mean sea level pressure reached a value of about 985.7 hPa (Fig. 1c). At that time, a 500 hPa two-trough system prevailed over the Ionian Sea and Sidra Gulf and was associated with an absolute vorticity maximum of $40 \times 10^{-5}\,s^{-1}$ over Northeastern Lybia (Fig. 1d). At the upper troposphere, an intense 300 hPa jet of $90\,m\,s^{-1}$ was identified over the southern edge of the trough (not shown).

By 12:00 UTC on 22 January, the system was located over the Eastern Aegean Sea and the coastline of western Turkey (Fig. 1e) and had deepened to about 976.4 hPa. This value is close to the minimum mean sea-level pressure of 977 hPa that was reported at the time by the nearby station of Samos Island (Lagouvardos et al., 2007). Considering that the cyclone moved at a mean latitude of about 36° N, the deepening of its central pressure by 22.5 hPa during the last 24 h corresponds to 1.42 bergerons. Therefore, this cyclone fulfils the criterion of Sanders and Gyakum (1980) and is upgraded to a bomb. In the middle troposphere the two troughs merged in one with the maximum absolute vorticity exceeding the $40 \times 10^{-5}\,s^{-1}$ over Cyprus (Fig. 1f).

3 Model characteristics and simulations design

3.1 Features of the model

The sensitivity of storm development and evolution to different lower boundary conditions has been investigated through the application of the Weather Research and Forecasting limited area model with the embedded dynamical core of Non-hydrostatic Mesoscale Model (WRF-NMM). The numerical simulations were performed on a single 305×273 domain with $0.09° \times 0.09°$ (almost 12 km) grid spacing and 38 vertical levels asymmetrically stretched up to 50 mb. The domain structure, which follows the Arakawa E-staggered grid, was centered at 39.50° N and 14.95° E (Fig. 2).

The model physics were based on the Ferrier microphysical scheme (Ferrier et al., 2002) for the grid scale cloud formation and precipitation. The latter predicts changes in water vapor and condensate in the forms of cloud water, rain, cloud ice, and precipitation ice. For the sub-grid scale effects of convective and/or shallow clouds, the Betts-Miller-Janjic cumulus scheme has been employed (Janjic et al., 2001; Janjic, 2003). The surface layer physics has been parameterized with the Monin-Obukhov-Janjic scheme (Janjic, 1996, 2002). The surface layer scheme estimates friction velocities and exchange coefficients that enable the calculation of surface heat and moisture fluxes by the land-surface model and surface stress in the planetary boundary layer scheme. The land-surface model is the unified NOAH (Chen and Dudhia, 2001). This is a 4-layer soil temperature and moisture model with canopy moisture and snow cover prediction. It includes root zone, evapotranspiration, soil drainage, and runoff, taking into account vegetation categories, monthly vegetation fraction and soil texture. The scheme provides sensible and latent heat fluxes to the boundary-layer scheme. It additionally predicts soil ice and fractional snow cover effects, has an improved urban treatment and considers surface emissivity properties. The parameterization of turbulence in the planetary boundary layer and in the free atmosphere follows the Mellor-Yamada-Janjic Level 2.5 turbulence closure scheme (Mellor and Yamada, 1982, Janjic, 1996). The GFDL scheme is implemented for the estimation of both longwave and shortwave radiation fluxes. It follows the simplified exchange method of Schwarzkopf and Fels (1991), with calculation over spectral bands associated with carbon dioxide, water vapor, and ozone.

3.2 Features of the numerical experiments

In an effort to examine the synoptic and mesoscale atmospheric response to different SST sources, five experiments were carried out. The simulation period extended from 21 January 2004 at 00:00 UTC (that is, 12 h before the formation of the cyclone and 36 h before the bomb reached its minimum sea-level pressure) to 23 January at 00:00 UTC. The entire set of simulations was based on identical atmospheric initial and lateral boundary conditions produced by ECMWF operational analyses. Analysis fields by the ECMWF at a $0.50° \times 0.50°$ (about 45×56 km) horizontal grid increment and 11 isobaric levels in the vertical were also used for the definition of the model initial and boundary conditions. The time increment of ECMWF analyses was set on a 6 h basis on the main synoptic hours (00:00, 06:00, 12:00 and 18:00 UTC). The first experiment, considered as the control simulation,

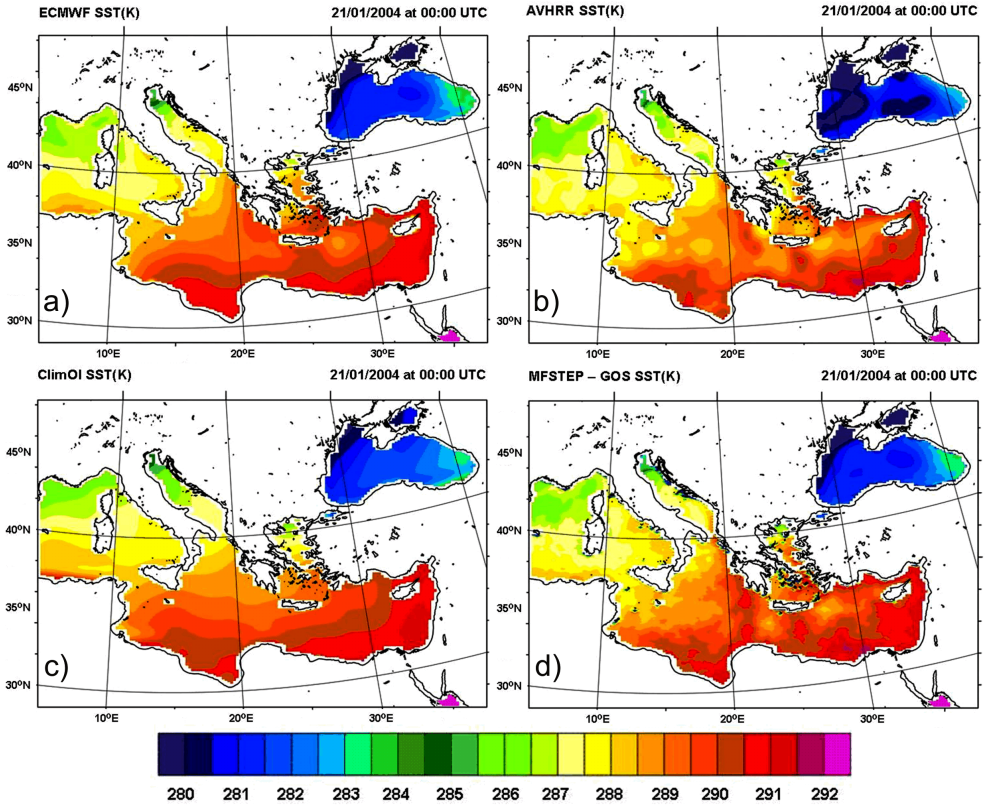

Fig. 3. Horizontal distribution of the sea surface temperature (°K) of 21 January 2004 at 00:00 UTC based on **(a)** ECMWF analysis, **(b)** AVHRR infrared satellite data, **(c)** NOAA 30-yr monthly climatology and **(d)** optimally interpolated GOS reanalysis.

Table 1. The experiments and the characteristics of the sea surface temperature data.

Experiment	Sea surface temperature source	Horizontal resolution (deg-km)	Temporal increment
1. ECMWF-SST	ECMWF operational analysis SST	$0.50° \times 0.50°$ ($\sim 46 \times 56$ km)	Daily average
2. AVHRR-SST	AVHRR infrared satellite SST	$0.25° \times 0.25°$ ($\sim 23 \times 28$ km)	Daily average
3. ClimOI-SST	NOAA Optimum Interpolation SST V2	$1.0° \times 1.0°$ ($\sim 91 \times 111$ km)	Monthly average
4. GOS-SST	Optimally interpolated re-analysis SST	$0.0625° \times 0.0625°$ ($\sim 5.7 \times 6.9$ km)	Daily average
5. ART-SST	Artificially constructed SST based on ECMWF operational analysis uniformly increased by 3 °K	$0.50° \times 0.50°$ ($\sim 46 \times 56$ km)	Daily average

consisted of ECMWF analysis SST data on $0.50° \times 0.50°$ horizontal resolution and henceforth, it will be referenced as ECMWF-SST. Figure 3a depicts the spatial distribution of ECMWF-SST at the time of model initialization and due to the coarse horizontal resolution, only large scale Mediterranean circulations were resolved. The second experiment was based on the Advanced Very High Resolution Radiometer infrared satellite SST data (hereafter AVHRR-SST) on $0.25° \times 0.25°$ horizontal grid increment with temporal resolution of one day. AVHRR SST is a daily average product that is bias adjusted using a spatially smoothed 7-day in situ SST average (Reynolds et al., 2007). Due to the

Table 2. The central mean sea level pressure (hPa) and the deepening rate (Bergeron) of the system in the five numerical simulations (ECMWF-SST, AVHRR-SST, CLIM-SST, GOS-SST and ART-SST) from 12:00 UTC on 21 January to 12:00 UTC on 22 January 2004. The last row of the table presents the central mean sea level pressure (hPa) and the deepening rate (Bergeron) of the system based on the ECMWF analysis.

Experiment	21 January 2004				22 January 2004					Deepening Rate
	12:00	15:00	18:00	21:00	00:00	03:00	06:00	09:00	12:00	
1.ECMWF-SST	996.1	996.8	995.8	991.2	987.0	983.4	979.6	975.4	974.1	1.43
2. AVHRR-SST	996.2	996.8	995.6	991.0	986.9	983.5	979.7	975.8	974.6	1.40
3. CLIM-SST	996.1	996.8	995.7	991.2	987.1	983.8	980.0	975.9	974.7	1.39
4. GOS-SST	996.1	996.8	995.7	991.1	986.9	983.3	979.2	975.7	974.4	1.41
5. ART-SST	996.1	996.4	995.2	990.4	986.2	982.8	978.1	974.0	973.6	1.43
ECMWF analysis	998.9	–	993.2	–	985.7	–	982.1	–	976.4	1.42

finer horizontal resolution, higher frequencies of the Mediterranean circulations were adequately resolved revealing significant temperature gradients over the Ionian and Libyan Seas (Fig. 3b). 30-yr monthly climatology (1971–2000) derived from the National Oceanic and Atmospheric Administration (NOAA) Optimum Interpolation SST V2 product (Reynolds et al., 2002) on the coarser $1^\circ \times 1^\circ$ horizontal resolution (Fig. 3c) was applied in the framework of the third experiment (hereafter ClimOI-SST). The fourth experiment was based on the optimally interpolated re-analysis SST data provided by the Gruppo di Oceanographia da Satellite (GOS) in the framework of the MFSTEP project (hereafter GOS-SST). The data has a temporal increment of one day and covers the Eastern Atlantic and the Mediterranean area on a very high horizontal resolution of $0.0625^\circ \times 0.0625^\circ$ (about 6×7 km). For the production of the GOS-SST, a complete re-analysis and interpolation on the MFSTEP OGCM (Ocean General Circulation Model) grid of the AVHRR SST measurements from 1985 to 2005 was performed (Marullo et al., 2007). In the GOS-SST, mesoscale patterns of Mediterranean circulations were resolved exhibiting meridional gradients of almost 0.6 °K/deg over the Ionian and Libyan Seas. Indeed, a narrow strip of prominent temperature gradient was located over the Southern Ionian Sea and according to Sanders (1986), it is a favourable marine environment for rapid storm development, since meteorological bombs are assumed baroclinic disturbances forced by a deep convective flux of latent and sensible heat received from the sea surface (Fig. 3d).

An additional experiment was conducted to assess the sensitivity of the system to an extreme and non-realistic surface forcing. Thus, a perturbed SST was developed using as a background field the ECMWF analysis SST uniformly increased by +3 °K for the entire computational domain. The artificially constructed SST (hereafter ART-SST) was applied as a lower boundary condition on $0.50^\circ \times 0.50^\circ$ horizontal resolution and the initial and lateral boundary conditions of the experiment were based on ECMWF operational analyses.

The SST sources and their characteristics for the five experiments of this study are described in Table 1 and comparative plots of the ECMWF SST deviations from the AVHRR, ClimOI and GOS SSTs are presented in Fig. 4. The comparison between the ECMWF and AVHRR SSTs revealed locally noticeable differences over the Eastern Mediterranean (Fig. 4a). Indeed, a maximum temperature deviation of +1.5 °K of the warmest ECMWF SST was evident over the Southern Mediterranean Sea from the Gulf of Sidra to the southern coastline of Crete, while the largest differences (up to about +2.0 °K) appeared locally over the Aegean Sea between Peloponnesus (southern Greek mainland) and the northern coastline of Crete. Local maxima were also evident at the central Aegean Sea, as well as close to the northwestern coastline of Cyprus. Temperature deviations of ECMWF analyses from ClimOI SST were even smaller (Fig. 4b) with most of the values ranging between −0.5 °K and +0.5 °K. Positive differences showed a warm bias of the ECMWF SST with local maxima (up to +1.5 °K) to be located around the Greek Peninsula and especially over the eastern Aegean Sea. The comparison between the ECMWF and the high resolution GOS SSTs revealed an extended area of negative differences up to −1.5 °K, locally appearing over the Ionian and Libyan Seas (Fig. 4c). Finally, the most prominent spatially distributed differences appeared between the AVHRR and GOS SSTs. Indeed, the systematically warmer GOS SST compared to the AVHRR SST revealed greater and more widespread temperature differences (locally exceeding the −2.0 °K) over the entire eastern Mediterranean Sea (Fig. 4d).

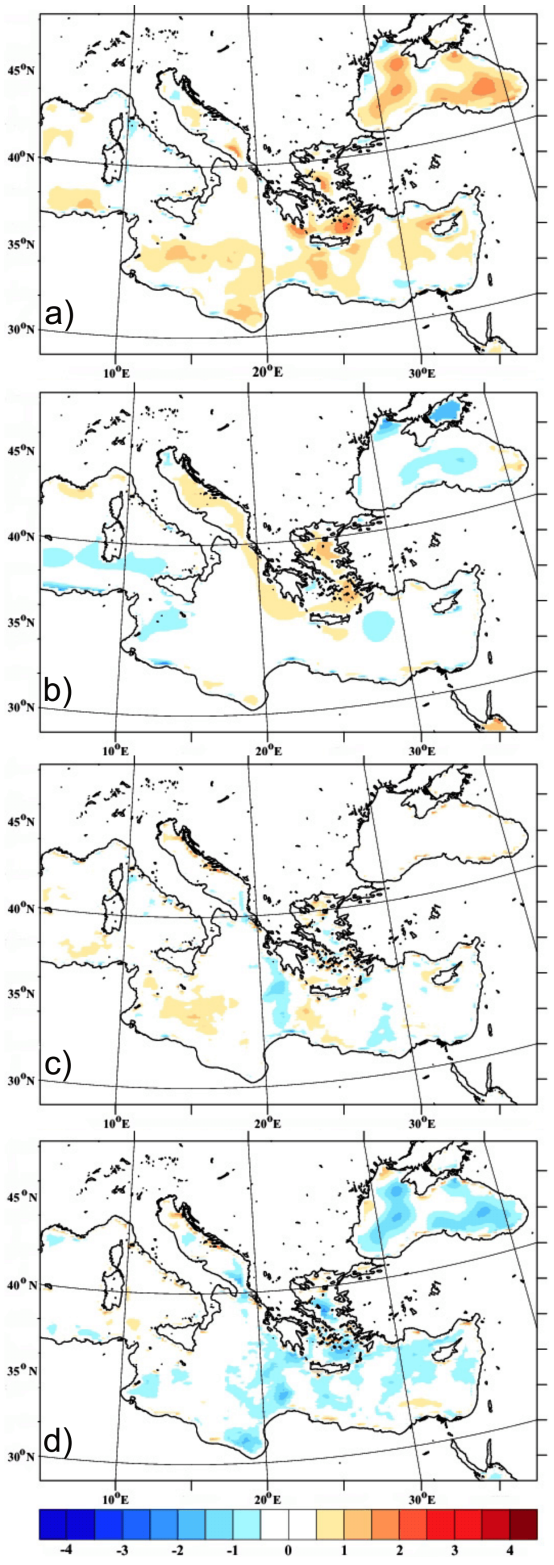

Fig. 4. Maps of the difference (in °K) between the **(a)** ECMWF and the AVHRR SSTs, **(b)** ECMWF and the ClimOI SSTs, **(c)** ECMWF and the GOS SSTs, and **(d)** AVHRR and the GOS SSTs valid at 00:00 UTC, 21 January 2004. Positive values indicate areas of warmer SSTs in the former dataset.

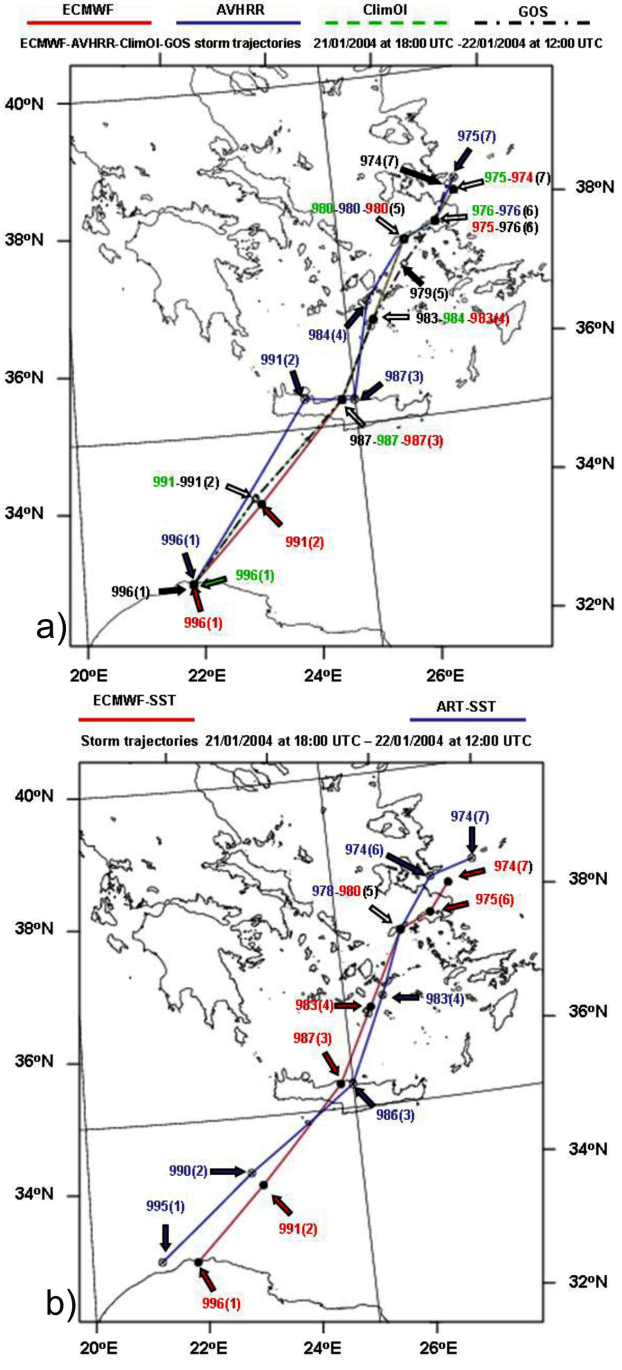

Fig. 5. Simulated storm tracks of the experiments **(a)** ECMWF-SST, AVHRR-SST, ClimOI-SST and GOS-SST, and **(b)** ECMWF-SST and ART-SST valid from 18:00 UTC 21 January 2004 to 12:00 UTC 22 January 2004 with 3-h time increment (7 time spots). The labels indicate the central mean sea level pressure (hPa) of the system and the values in the parentheses denote the relevant time spots.

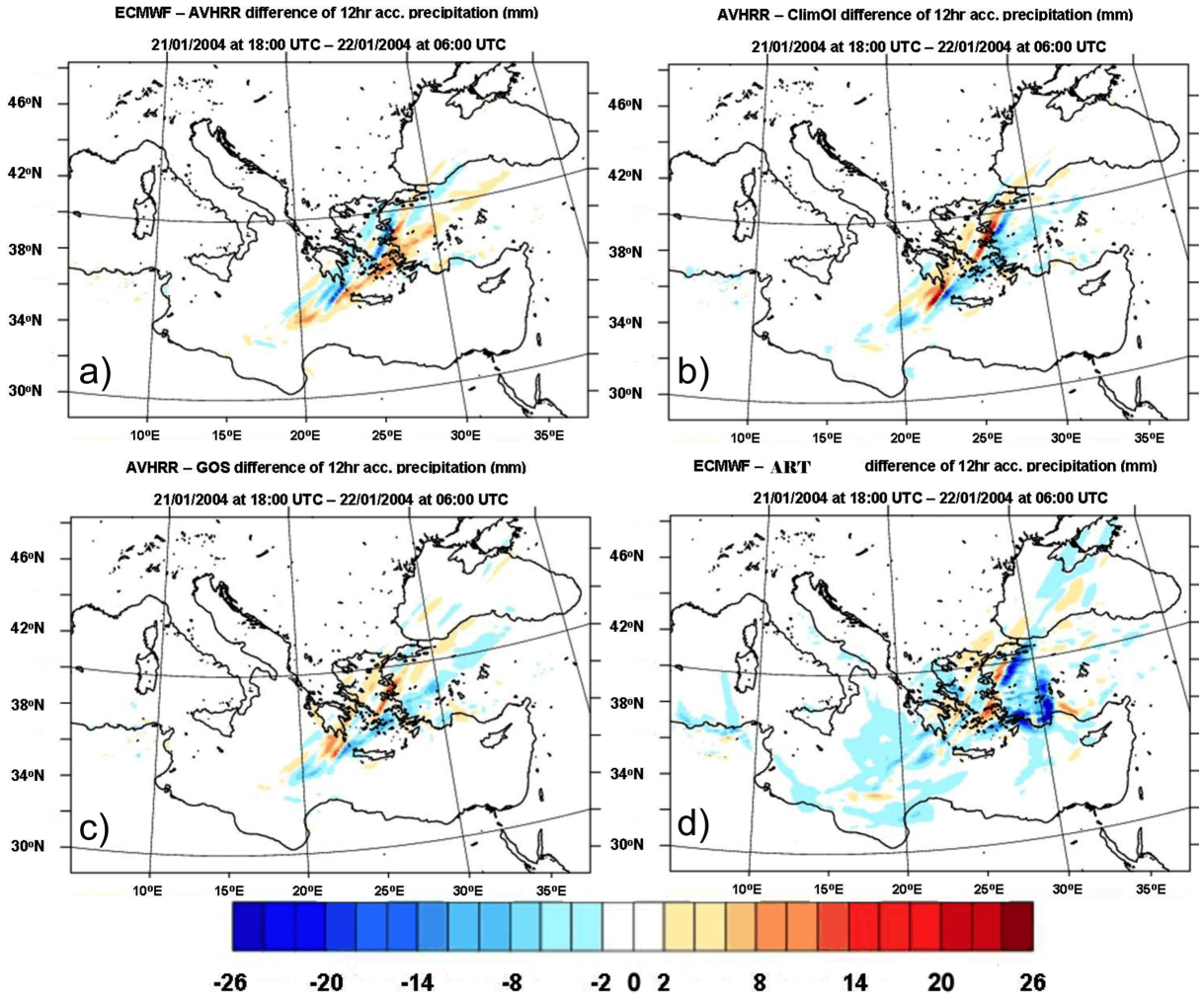

Fig. 6. Maps of difference of the 12-h accumulated precipitation (mm) over Greece between the experiments: **(a)** ECMWF-SST and AVHRR-SST, **(b)** AVHRR-SST and ClimOI-SST, **(c)** AVHRR-SST and GOS-SST and **(d)** ECMWF-SST and ART-SST for the period 18:00 UTC, 21 January 2004 to 06:00 UTC, 22 January 2004. Values in the range ± 2 mm are masked white.

4 Analysis of the numerical experiments

As it is shown in Table 2, the sensitivity of storm development in the five experiments gets initially expressed in terms of storm central mean sea-level pressure (SCP). Based on the model output, the SCP has been estimated on a three hour basis starting from 21 January 2004 at 12:00 UTC till 22 January 2004 at 12:00 UTC. This period was chosen because it appropriately describes the explosive cyclogenesis of the system and its passage over the Aegean Sea.

Comparing the ECMWF analysis data on 22 January 2004 at 00:00 UTC to the first four simulations, the latter showed higher SCP values ranging from 986.9 to 987.1 hPa instead of 985.7 hPa (Table 2). Twelve hours later, when the system reached its minimum SCP, the conventional meteorological station located at Samos Island (Eastern Aegean Sea) recorded a mean sea level pressure of 977 hPa, while the model-generated SCPs for the grid point nearest to Samos ranged from 974.1 to 974.7 hPa. At that time, the fifth experiment based on the artificially constructed SST (ART-SST) simulated a slightly deeper system with SCP equal to 973.6 hPa. Furthermore, the deepening rates in the four experiments ranged from 1.39 to 1.43 bergerons, a value most close to that of 1.42 appearing in the ECMWF analyses. The ART-SST simulation produced a similar deepening rate with 1.43 bergerons. Such basic evaluation shows that the model was able to resolve the main synoptic evolution of the bomb, represented by the SCP that characterizes this kind of rapidly developing system. However, a more detailed and comprehensive evaluation follows in the next section.

The simulated storm tracks were extracted on the basis of 3-hourly SCP values, from 21 January 2004 at 18:00 UTC to 22 January 2004 at 12:00 UTC (7 time spots). In Fig. 5a the colored lines illustrate how the four realistic experiments

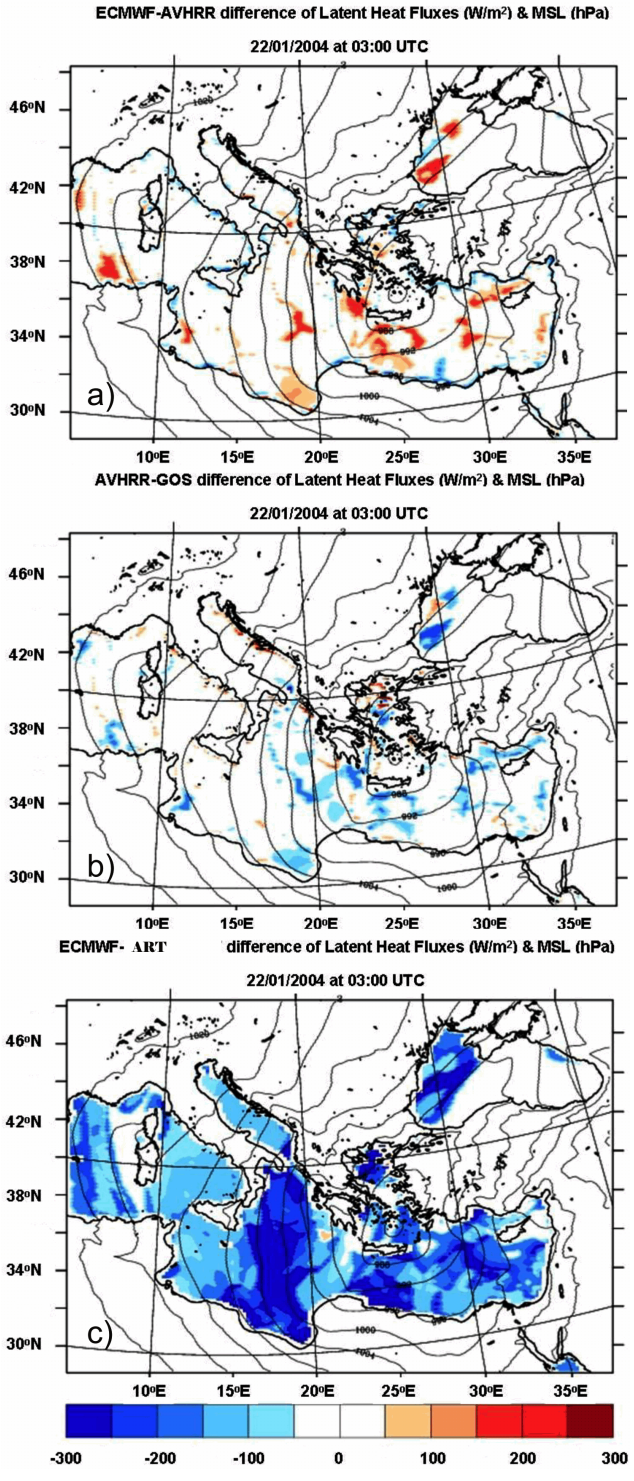

Fig. 7. Maps of the difference of the surface latent heat flux ($W\,m^{-2}$) between **(a)** ECMWF-SST and AVHRR-SST, **(b)** AVHRR-SST and GOS-SST and **(c)** ECMWF-SST and ART-SST simulations, valid at 03:00 UTC on 22 January 2004. Values in the range $\pm 50\,W\,m^{-2}$ are masked white. The contour lines denote the mean sea level pressure (hPa) in the control (ECMWF-SST) experiment.

simulated the track of the storm. More specifically, the blue solid line corresponds to the storm track simulated in the AVHRR-SST experiment, the red solid line corresponds to the ECMWF-SST track, the green dashed line denotes the ClimOI-SST track and the black dot-dashed line corresponds to the GOS-SST track. The blue, green, red and black labels refer to the SCP values as they were extracted from the AVHRR-SST, ClimOI-SST, ECMWF-SST and GOS-SST experiments respectively. As it is shown, storm tracks and SCPs simulated by the ECMWF-SST and ClimOI-SST were almost identical for the defined 3-hourly time spots, while small but noticeable and not systematic deviations of the track were estimated by the AVHRR-SST. The simulation forced by the high resolution GOS-SST produced almost negligible deviations on the storm track and the SCP compares to both the ECMWF-SST and ClimOI-SST experiments. Such similarities across the four experiments indicate that the SST data source had a limited impact on the intensity and location of the storm.

Comparing the storm tracks and SCPs patterns simulated by the ECMWF-SST and ART-SST experiments, one does not fail to notice their strong similarity (Fig. 5b). The significant perturbation of the ECMWF SST with an unrealistic and uniform increase of +3 °K did not result in a different track of the storm while the maximum difference of the SCPs was just up to 1.5 hPa on 22 January at 06:00 UTC (Table 2). These similarities have also been documented by McInnes et al. (1992) through the investigation of cut-off lows and their sensitivity to sea-surface temperature conditions.

Despite such a small response to the storm track and the SCP, more detailed investigation indicated the existence of spatiotemporal deviations in the distribution of precipitation due to the implementation of different SST sources. The differences in the 12-h (18:00 UTC, 21 January 2004 to 06:00 UTC, 22 January 2004) accumulated precipitation between the first four experiments are plotted in Fig. 6 and indicate that the maximum precipitation amount remained almost insensitive to the different SSTs. Although the different sea-surface forcing produced limited response to the transition speed of the system and the amount of precipitation, it significantly influenced the spatial distribution of the rainbands. Thus, the ECMWF-SST experiment placed the main cores of precipitation southeasterly of those simulated by the AVHRR-SST experiment (Fig. 6a). Similarly, ClimOI-SST exhibited a significant shift of the simulated rainbands compared to those estimated by AVHRR-SST (Fig. 6b). Furthermore the GOS-SST experiment shifted the simulated precipitation to a southeasterly direction compared to the one simulated by AVHRR-SST (Fig. 6c).

However, the artificially constructed SSTs prominently affected both the simulated spatiotemporal distribution of precipitation and the local rain maxima (Fig. 6d). Comparing against the ECMWF-SST experiment (control run), ART-SST produced a more widespread spatial structure of the precipitation and moved the main cores of the rain towards a

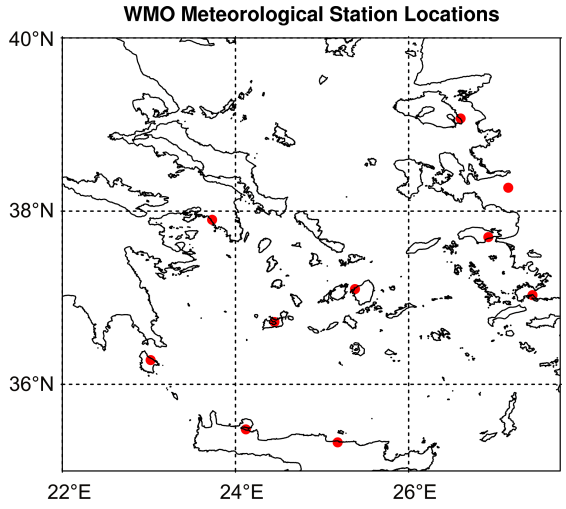

Fig. 8. Locations of the World Meteorological Organization (WMO) stations used in the statistical evaluation.

southeastern direction. The displacement of the rainbands appearing in the various experiments that utilized identical initial and boundary conditions everywhere but on the sea-surface, is possibly associated with the surface heat fluxes. Furthermore, warmer SSTs induce stronger vertical momentum mixing, which is responsible for mesoscale features in the surface wind convergence field (Xie, 2004; Chelton et al., 2004). Indeed, Fig. 7a and b show that the ECMWF-SST and GOS-SST experiments induced stronger upward latent heat fluxes than AVHRR-SST with differences exceeding 150 W m^{-2}. The local maxima of the latent heat flux differences were mainly located over the cold sector of the storm and almost collocated with the SST anomalies in Fig. 4a and d, supplying the system with excess energy. Such results further prove that the warmer the SSTs, the more prominent the surface fluxes become. Figure 7c shows that the perturbed SST induced stronger upward latent heat fluxes compared to the control run, producing a significantly more unstable marine boundary layer. The latent heat flux differences reached 300 W m^{-2} in extended regions of the Central-Eastern Mediterranean. In summary, the stronger boundary layer destabilization in the ART-SST experiment affected prominently both the simulated spatiotemporal distribution and the local maxima of precipitation, but not the SCP and the storm track.

5 Statistical verification

The impact of the different SST forcing on model performance has been finally evaluated using a statistically based methodology. The aim was to provide a quantitative assessment of the model response to different lower boundary forcing. To this end, observational data from 10 conventional stations in the vicinity of the storm track (Fig. 8) were used to verify and compare categorical model forecasts for both continuous (mean sea level pressure and wind speed at 10 m) and discrete (precipitation) variables. The evaluation was carried out between 21 January at 12:00 UTC and 22 January at 18:00 UTC (that is during the intensification phase) and was based on point-to-point comparison between model-generated variables and observations. Therefore, 110 pairs of model estimated and observed values were extracted from each experiment for the predefined evaluation period. For the continuous variables, the produced scores were the standard mean error (bias) and the root mean square error (RMSE) (Wilks, 1995). The verification scores for the precipitation were BIAS and RMSE as well, and were derived using the contingency table approach (Papadopoulos and Katsafados, 2009).

Mean sea level pressure bias time-plots indicated that the bias values of both ECMWF-SST and ClimOI-SST were almost similar throughout the evaluation period and in general, they were smaller that the mean errors of the AVHRR-SST and GOS-SST simulations (Fig. 9a). Furthermore, RMSE properties revealed an increasing trend over time which has been more prominent in the AVHRR-SST and GOS-SST experiments (Fig. 9b). The ECMWF-SST and ClimOI-SST produced lower errors than the other two experiments in the second half of the simulation period when the system reached maximum intensity. In contrast to the mean sea level pressure, all four simulations overestimated the wind speed at 10 m with a bias peak of 4.5 m s^{-1} on January 22 at 06:00 UTC (Fig. 9c), which is associated with increased RMSE scores up to 5.5 m s^{-1} (Fig. 9d). The increased bias and RMSE scores of the wind speed are related to the misplacement of the system, especially at the time of entering in the Aegean Sea which is possibly attributed to the poor representation of the complex terrain and the existence of small islands there. However, the GOS-SST experiment showed overall improved scores at a range of 10–15% than those estimated by the rest simulations during the entire period of evaluation. Figure 9e illustrates that small precipitation thresholds (0.5–6 mm) in all four experiments were slightly overestimated whthe GOS-SST showed reduced overestimation of the lower precipitation thresholds and the ECMWF-SST produced the lowest underestimation in the range of thresholds exceeding 6.0 mm. However the RMSE values were almost similar for all thresholds across the four experiments (Fig. 9f).

The above scores revealed that the different SST sources produced noticeable effects on the model's performance. Indeed, the ECMWF-SST experiment slightly outperformed the simulation forced by a higher horizontal resolution SST, namely the AVHRR-SST. This can mainly be attributed to the balanced fields supported by the ECMWF, as they were produced from advanced data assimilation schemes enriched with satellite retrievals and a number of sea surface observational data (e.g. buoys, drifters etc). In addition, the very high resolution GOS SST was able, owing to the adequate

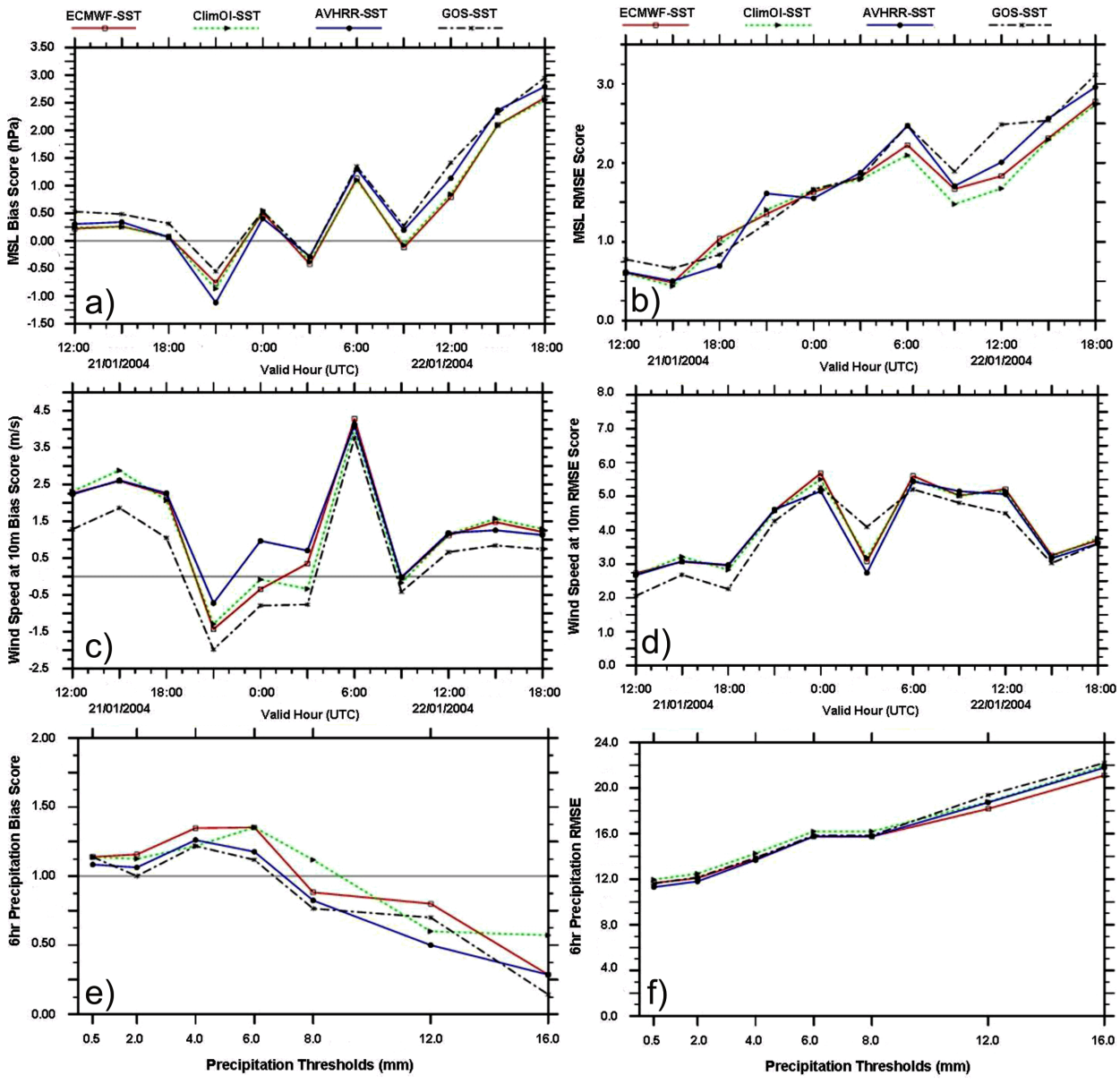

Fig. 9. Time plots of the bias scores (**a, c** and **e**) and RMSE scores (**b, d** and **f**) of the mean sea level pressure (hPa), the wind speed at 10 m ($m\,s^{-1}$) and the 6-hourly accumulated precipitation (mm) respectively across the ECMWF-SST (solid red line), AVHRR-SST (solid blue line), ClimOI-SST (green dashed line) and GOS-SST (black dot-dashed line) experiments for the period 12:00 UTC, 21 January 2004 to 18:00 UTC, 22 January 2004.

representation of the mesoscale oceanic features, to produce a rather moderate improvement on the wind speed and the precipitation skill scores. However the results of the statistical evaluation for this specific case can not characterize the quality of the applied high-resolution SSTs in general since their impact on the forecasting and hindcasting skill of the numerical models has been well documented in the literature (e.g. Castellari et al., 2000; Natale et al., 2006).

6 Concluding remarks and discussion

The sensitivity of a storm development in marine environment and its intensity to different SST forcing has been analyzed through comparative numerical simulations. The case of an explosively developing storm over the Eastern Mediterranean on 21–22 January 2004 was selected in view of its intensity and severe effects. The methodology consisted of four comparative simulations based on identical atmospheric initial and boundary conditions, but different SST

forcing (ECMWF analysis, AVHRR satellite-derived, GOS optimally interpolated re-analysis and 30-year monthly climatology SST data) to be applied as lower boundary conditions. Furthermore, an additional experiment was conducted in order to assess the sensitivity of the system to an extreme and non-realistic surface forcing (ART-SST). The artificially constructed SST was based on the ECMWF analysis SST uniformly increased by +3 °K for the entire computational domain.

Despite the fact that the storm was supported with an additional latent heat flux up to 150 W m^{-2}, especially in the case of the ECMWF-SST simulation, all four realistic numerical experiments revealed a rather insensitive system to sea surface conditions and processes. Thus, the impact of the four different SST fields was to produce different storm central mean sea level pressures (SCPs) by values ranging between 0.1 and 0.8 hPa. Turning to the spatial organization of the system, the simulated storm paths remained almost unchanged among the four experiments. In addition ART-SST simulation induced stronger upward latent heat fluxes, with differences locally exceeding by 300 W m^{-2} the ones of ECMWF-SST, and its impact was to deepen the SCP up to 1.5 hPa.

The abovementioned similarities indicate that surface fluxes did not play a primary role in the development of the meteorological bomb (in agreement with Lagouvardos et al., 2007) and that they had a limited impact on the intensity and the location of the storm, differentiating it from some "tropical cyclone"-like Mediterranean storms in which the Wind Induced Surface Heat Exchange mechanism (e.g. Emanuel, 1986; Craig and Gray, 1996) assumes a primary role (Pytharoulis et al., 2000). The system was mainly controlled by the upper air atmospheric conditions, because its rapid development was mainly associated with a two-trough system which, under the influence of a very intense upper-level jet, was merged into one. However, the existence of spatiotemporal deviations on the distribution of precipitation could be characterized as the most significant response to the different sea-surface forcing. The displacement of the rainbands appearing in the various experiments can possibly be associated with the simulated surface heat fluxes that induce stronger vertical momentum mixing responsible for mesoscale features in the surface wind convergence field.

The model's performance and its response to the different lower boundary forcing, has been also statistically assessed. This assessment was carried out using surface data from conventional weather observing stations across the track of the storm. According to the statistical scores, a systematic overestimation of the mean sea-level pressure and the wind speed at 10 m, as well as an underestimation of high precipitation rates (>8 mm/6 h), characterized all experiments. In particular, the GOS-SST experiment showed an overall improvement of the wind speed estimation at a range of 10–15% during the entire period of evaluation. However, the ECMWF-SST and ClimOI-SST simulations exhibited almost similar accuracy and slightly better skill scores than the AVHRR-SST experiment. The results obtained reveal the possible limitations of the imposed satellite-derived and on a higher horizontal resolution AVHRR SST. The ECMWF SST was able to reproduce the model's lower boundary forcing in a more efficient manner by assimilating a number of in-situ sea surface observational data. The simulation forced by the high resolution GOS SST outperformed the AVHRR-SST in most cases, showing reduced overestimation in the lower precipitation thresholds (up to 6 mm). Although the abovementioned diagnoses indicate a rather weak role of SSTs in the intensity and the characteristics of this deep Mediterranean storm, additional simulations with advanced nudging methods covering more case studies and under various synoptic conditions are in the authors' near future plans.

Acknowledgements. One of the authors, E. Mavromatidis, owes special thanks to the Hellenic Ministry of Education Lifelong Learning and Religious Affairs for providing him with the absence of leave that enabled him to complete this study. The European Centre for Medium Range Weather Forecasts (ECMWF) is gratefully acknowledged for the provision of gridded analyses and surface observational data. The National Climatic Data Center (NCDC) and the Climate Prediction Center (CPC) of National Oceanic and Atmospheric Administration (NOAA) are acknowledged for the making the Advanced Very High Resolution Radiometer (AVHRR) satellite products, and the 30-yr monthly climatology sea surface temperature data, respectively, available. We would also like to acknowledge the Gruppo di Oceanographia da Satellite (GOS) of Istituto di Scienze dell'Atmosfera e del Clima (ISAC) for the provision of the re-analysis sea surface temperature data (http://gos.ifa.rm.cnr.it). Finally, the authors would like to thank K. Lagouvardos for his helpful comments on this manuscript and the four anonymous reviewers for providing insightful suggestions that enhanced the scope and quality of the article.

Edited by: J. Salat
Reviewed by: J. A. Garcia-Moya, K. Lagouvardos, and three other anonymous referees

References

Capaldo, M., Conte, M., Finizio, C., and Todisco, G.: A detailed analysis of a severe storm in the central Mediterranean: the case of the Trapani Flood, Rivista di Meteorologia Aeronautica, XL, 183–199, 1980.

Castellari, S., Pinardi, N., and Leaman, K.: Simulation of water mass formation proces in the Mediterranean Sea: Influence of the time frequency of the atmospheric forcing, J. Geophys. Res., 105(C10), 24157–24181, 2000.

Chelton, D. B., Schlax, M. G., Freilich, M. H., and Milliff, R. F.: Satellite measurements reveal persistent small-scale features in ocean winds, Science, 303, 978–983, 2004.

Chen, F. and Dudhia, J.: Coupling an advanced land-surface/hydrology model with the Penn State/NCAR MM5 modeling system. Part I: Model implementation and sensitivity, Mon. Weather. Rev., 129 (4), 569–585, 2001.

Conte, M., Sorani, R., and Piervitali, E.: Extreme Climatic Events over the Mediterranean, in: Mediterranean desertification: a mosaic of processes and responses. edited by: Geeson, N. A., Brandt, C. J., and Thornes, J. B., Wiley & Sons, Ltd. Pp. 15–31, 2002.

Craig, G. C. and Gray, S. L.: CISK or WISHE as the mechanism for tropical cyclone intensification, J. Atmos. Sci., 53, 3528–3540, 1996.

Emanuel, K. A.: An Air-Sea Interaction Theory for Tropical Cyclones. Part I: Steady-State Maintenance, J. Atmos. Sci., 43, 585–604, 1986.

Ferrier, B. S., Jin, Y., Lin, Y., Black, T., Rogers, E., and DiMego, G.: Implementation of a new grid-scale cloud and precipitation scheme in the NCEP Eta model. Preprints, 15th Conf. On Numerical Weather Prediction, San Antonio, TX, Am. Meteor. Soc., 280–283, 2002.

Gyakum, J. R. and Danielson, R. E.: Analysis of meteorological precursors to ordinary and explosive cyclogenesis in the western north pacific, Mon. Weather Rev., 128, 851–863, 2000.

Hirose, N. and Fukudome, K.: Monitoring the Tsushima warm current improves seasonal prediction of the regional snowfall, Sci. Online Lett. Atmos., 2, 61–63, 2006.

Janjic, Z. I.: The Mellor-Yamada level 2.5 scheme in the NCEP Eta model, $11th$ Conf. On Numerical Weather Prediction, Norfolk, VA, 19–23 August 1996, Am. Meteor. Soc., Boston, MA, 354–355, 1996.

Janjic, Z. I., Gerrity J. P. Jr, and Nickovic, S.: An alternative approach to nonhydrostatic modelling, Mon. Weather Rev., 129, 1164–1178, 2001.

Janjic, Z. I.: Nonsingular Implementation of the Mellor–Yamada Level 2.5 Scheme in the NCEP Meso model, NCEP Office Note, 437, 61 pp., 2002.

Janjic, Z. I.: A nonhydrostatic model based on a new approach, Meteorol. Atmos. Phys., 82, 271–285, doi:10.1007/s00703-001-0587-6, 2003.

Karacostas, T. S. and Flocas, A. A.: The development of the "bomb" over the Mediterranean area, La Meteorologie, 34, 351–358, 1983.

Kathleen, M. C. and Capehart, W. J.: Sensitivity of medium-range forecasts in WRF to Sea Surface Temperatures, 9th WRF Users Workshop, 23–27 June 2008, Boulder, Colorado, 2008.

Kushnir, Y., Robinson, W. A., I. Blade, N., Hall, M. J., Peng, S., and Sutton, R.: Atmospheric GCM response to extratropical SST anomalies: Synthesis and evaluation, J. Clim., 15, 2233–2256, 2002.

Lagouvardos K., Kotroni, V., Nickovic, S., Jovic, D., Kallos, G., and Tremback, C. J.: Observations and model simulations of a winter sub-synoptic vortex over the central Mediterranean, Met. Apps., 6, 371–383, 1999.

Lagouvardos, K., Kotroni, V., and Defer, E.: The 21–22 January 2004 explosive cyclogenesis over the Aegean Sea: Observations and model analysis, Q. J. R. Meteorol. Soc., 133, 1519–1531, doi:10.1002/qj.121, 2007.

Lebeaupin Brossier, C., Ducrocq, V., and Giordani, H.: Effects of the air – sea coupling time frequency on the ocean response during Mediterranean intense events, Ocean Dyn., 59, 539–549, doi:10.1007/s10236-009-0198-1, 2009.

Liu, Z. and Wu, L.: Atmospheric response to North Pacific SST anomaly: The role of ocean-atmosphere coupling, J. Clim., 17, 1859–1882, 2004.

Macdonald, B. and Reiter, E. R.: Explosive Cyclogenesis over the Eastern United States, Mon. Weather Rev., 116, 1568–1586, 1988.

Martin, J. E. and Otkin, J. A.: The rapid growth and decay of an extratropical cyclone over the central Pacific Ocean, Wea. Forecast., 19, 358–376, 2004.

Marullo, S., Nardelli, B. B., Guarracino, M., and Santoleri, R.: Observing the Mediterranean Sea from space: 21 years of Pathfinder-AVHRR sea surface temperatures (1985 to 2005): reanalysis and validation, Ocean Sci., 3, 299–310, 2007, http://www.ocean-sci.net/3/299/2007/.

McInnes, K., Leslie, L. M., and McBride, J. L.: Numerical simulation of cut-off lows on the Australian east coast: Sensitivity to sea-surface temperature, Int. J. Clim., 12, 783–795, 1992.

Mellor, G. L. and Yamada, T.: Development of a turbulence closure model for geophysical fluid problems, Rev. Geophys. Space Phys., 20, 851–875, 1982.

Millán, M., Estrela, M. J., and Caselles, V.: Torrential precipitations on the Spanish east coast: The role of the Mediterranean sea surface temperature, Atm. Res., 36, 1–16, 1995.

Natale, S., Sorgente, R., Gaberšek, S., Ribotti, A., and Olita, A.: Central Mediterranean Sea forecast: effects of high-resolution atmospheric forcings, Ocean Sci. Discuss., 3, 637–669, doi:10.5194/osd-3-637-2006, 2006.

Minobe, S., Kuwano-Yoshida, A., Komori, N., Xie, S. P., and Small, R. J.: Influence of the Gulf Stream on the troposphere, Nature, 452, 206–209, doi:10.1038/nature06690, 2008.

Pandolfo, J. P.: Preliminary estimates of the role of mesosynoptic scale sea surface temperature features in fostering explosive midlatitude cyclogenesis, Mon. Weather Rev., 113, 1417–1420, 1985.

Papadopoulos, A. and Katsafados, P.: Verification of operational weather forecasts from the POSEIDON system across the Eastern Mediterranean, Nat. Hazards Earth Syst. Sci., 9, 1299–1306, doi:10.5194/nhess-9-1299-2009, 2009.

Pastor F., Estrela, M. J., Penarrocha, D., and Millán, M. M.: Torrential rains on the Spanish Mediterranean coast: Modelling the effects of the sea surface temperature, J. App. Met., 40, 1180–1194, 2001.

Pytharoulis I., Craig, G. C., and Ballard, S. P.: The hurricane-like Mediterranean cyclone of January 1995, Met. Apps., 3, 261–279, 2000.

Reynolds, R. W., Rayner, N. A., Smith, T. M., Stokes, D. C., and Wang, W.: An Improved In Situ and Satellite SST Analysis for Climate, J. Climate, 15, 1609–1625, 2002.

Reynolds, R. W., Smith, T. M., Liu, C., Chelton, D. B., Casey, K. S., and Schlax, M. G.: Daily High-Resolution-Blended Analyses for Sea Surface Temperature, J. Climate, 20, 5473–5496, doi:10.1175/2007JCLI1824.1., 2007.

Rouault, M., White, S. A., Reason, C. J. C., Lutjeharms, J. R. E., and Jobard, I.: Ocean – Atmosphere Interaction in the Agulhas Current Region and a South African Extreme Weather Event, Wea. Forecasting, 17, 655–669, 2002.

Rouault, M., Reason, C. J. C., Lutjeharms, J. R. E., and Beljaars, A. C. M.: Underestimation of latent and sensible heat fluxes above the Agulhas Current in NCEP and ECMWF analyses, J. Climate, 16, 776–782, 2003.

Sanders, F.: Explosive cyclogenesis in the west-central North At-

lantic Ocean, 1981–1984, Part I: Composite structure and mean behavior, Mon. Weather Rev., 114, 1781–1794, 1986.

Sanders, F. and Gyakum, J. R.: Synoptic-dynamic climatology of the bomb, Mon. Weather Rev., 108, 1589–1606, 1980.

Schwarzkopf, M. D. and Fels, S. B.: The simplified exchange method revisited. An accurate, rapid method for computation of infrared cooling rates and fluxes, J. Geophys. Res., 96 (D5), 9075–9096, 1991.

Strahl, J. L. and Smith, P. J.: A diagnostic study of an explosively developing extratropical cyclone and an associated 500-hPa trough merger, Mon. Weather Rev., 129, 2310–2328, 2001.

Sutton, R. and Mathieu, P.: Response of the atmosphere-ocean mixed layer system to anomalous ocean heat flux convergence, Q. J. R. Meteorol. Soc., 128, 1259–1275, 2002.

Wilks, D. S.: Statistical methods in the atmospheric sciences: An introduction, Academic Press, San Diego, California, 467 pp., 1995.

Xie, S. P.: Satellite observations of cool ocean-atmosphere interaction, Bull. Am. Met. Soc., 85, 195–208, 2004.

Yamamoto, M., and Hirose, N.: Impact of SST reanalyzed using OGCM on weather simulation: A case of developing cyclone in the Japan Sea area, Geophys. Res. Lett., 34, L005808, doi:10.1029/2006GL028386, 2007.

Yulaeva, E., Schneider, N., Pierce, D., and Barnett, T.: Modeling of North Pacific climate variability forced by oceanic heat flux anomalies, J. Climate, 14, 4027–4046, 2001.